DOI: 10.1002/chem.200800147

Fluorescent, Synthetic Amphiphilic Heptapeptide Anion Transporters: Evidence for Self-Assembly and Membrane Localization in Liposomes

Lei You[b] and George W. Gokel*[a, b]

Abstract: Synthetic anion transporters (SATs) of the general type (n-$C_{18}H_{37})_2$N-$COCH_2OCH_2CO$-$(Gly)_3$-Pro-$(Gly)_3$-O-n-C_7H_{15}, **1**, are amphiphilic peptides that form anion-conducting pores in bilayer membranes. To better understand membrane insertion, assembly and aggregation dynamics, and membrane penetration, four novel fluorescent structures were prepared for use in both aqueous buffer and phospholipid bilayers. The fluorescent residues pyrene, indole, dansyl, and NBD were incorporated into **1** to give **2**, **3**, **4**, and **5**, respectively. Assembly of peptide amphiphiles in buffer was confirmed by monitoring changes in the pyrene monomer/excimer peaks observed for **2**. Solvent-dependent fluorescence changes that were observed for indole (**3**) and dansyl (**4**) side-chained SATs in bilayers showed that these residues experienced an environment between $\varepsilon = 9$ (CH_2Cl_2) and $\varepsilon =$ 24 (EtOH) in polarity. Fluorescence resonance energy transfer (FRET) between **2** and **3** demonstrated aggregation of SAT monomers within the bilayer. This self-assembly led to pore formation, which was detected as Cl^- release from the liposomes. The results of acrylamide quenching of fluorescent SATs supported membrane insertion. Studies with NBD-labeled SAT **5** showed that peptide partition into the bilayer is relatively slow. Dithionite quenching of NBD-SATs suggests that the amphiphilic peptides are primarily in the bilayer's outer leaflet. Images obtained by using a fluorescence microscope revealed membrane localization of a fluorescent SAT. Taken together, this study helps define the insertion, membrane localization, and aggregation behavior of this family of synthetic anion transporters in liposomal bilayers.

Keywords: anion transport · assembly · fluorescent probes · membranes · peptides · self-assembly

Introduction

A range of interesting and effective anion-complexing agents[1,2] has been reported in recent years.[3–7] Although there are fewer examples, some of these complexing agents have been studied as agents that mediate the flux of, for example, chloride through bilayer membranes.[8,9] Molecules have been designed to transport chloride by both carrier or pore-forming mechanisms.[10–14] The equilibrium complexation of anions by a receptor molecule can be characterized dynamically by solution-phase binding constant measurements and statically by X-ray crystallography. The characterization of synthetic anion transporters (SATs) that insert and function in bilayers presents a greater analytical challenge.

Molecules that bind ions may or may not function as transporters. They may transport ions by forming complexes of fixed or variable stoichiometry. Further, if they form pores or channels, they might not show significant binding for the ions whose transport they mediate. The extent of ion transport can be assayed in various ways, including ion release from liposomes, planar bilayer voltage-clamp studies, and bioactivity assessment.[15] Thus far, most studies have monitored transporter-mediated anion entry to or egress from liposomes. Fluorescent dyes (e.g. pyranine, lucigenin)[16,17] or ion-selective electrodes[18,19] can be used to detect ion flux. The transport mechanism (channel, pore, or carrier) and ion selectivity can both be assessed by using the

[a] Prof. Dr. G. W. Gokel
Departments of Chemistry & Biochemistry and Biology
Center for Nanoscience, University of Missouri–Saint Louis
One University Boulevard
Saint Louis, MO 63121 (USA)
Fax: (+1) 314-516-5342
E-mail: gokelg@umsl.edu

[b] L. You, Prof. Dr. G. W. Gokel
Department of Chemistry, Washington University
One Brookings Drive
Saint Louis, MO 63130 (USA)

Supporting information for this article is available on the WWW under http://www.chemeurj.org/ or from the author. It contains additional fluorescence data and synthetic procedures.

planar bilayer technique,[20] but it is both more cumbersome and time consuming than the measurement of ion release from liposomes. A further complication in monitoring ion flux is that not all release occurs smoothly or consistently. Thus, different curve shapes can be observed when continuous release is monitored over time.

When a synthetic anion transporter functions within a phospholipid bilayer, the process is potentially affected by a number of variables. One question is how readily and completely the SAT inserts into the bilayer.[21] A second question concerns how efficiently self-assembly of the inserted monomers occurs, and how effectively the aggregate forms a functional pore. If a pore forms by self-assembly, deaggregation can also occur as can transverse relaxation (monomer translocation, flip–flop).[22] Intervesicular transfer[23] of pore-forming elements can also affect transport efficacy. Identifying or confirming these processes is a challenge for peptides that are known to reside in membranes, but even more complicated for synthetic systems that can exhibit a broader range of behavior.

The SATs[24] that have been developed in our laboratory typically comprise seven amino acids, but may have either longer or shorter peptide sequences.[25] Planar bilayer conductance measurements showed ion selectivity of Cl^- over $K^+ > 10$-fold for the original compound.[24a] Evidence, such as Hill plots, suggests that the amphiphilic peptides function at least as dimers.[26] The preparation of functional *pseudo*-dimers is in concert with this inference.[27] The details of SAT aggregation in the bulk aqueous phase and aggregation or insertion in the bilayer remain unclear. In an effort to further define the behavior of SATs, we have extended studies with glutamate-containing peptide sequences[28] to fluorescent derivatives. Here we report the use of fluorescent transporters and a range of analytical techniques to assess the assembly, partition, and positions within the bilayer of our synthetic, amphiphilic peptide-based anion transporters.

Results and Discussion

Compounds studied: The twin octadecyl chains in our first SAT ($(C_{18}H_{37})_2$N-$COCH_2OCH_2CO$-$(Gly)_3$-Pro-$(Gly)_3$-OCH_2Ph)[24] were intended to mimic the fatty acid chains of phospholipid membrane monomers. The diglycolyl residue (-$COCH_2OCH_2CO$-) was introduced as a spacer between the anchor chains and the peptide. The position and polarity of the atoms in this spacer emulate the distances and the corresponding polar and nonpolar elements of the diacylglycerol subunit (the midpolar regime) in a typical phospholipid monomer. The half amide acid, $R_2NCOCH_2OCH_2COOH$, was then connected to the N terminus of the heptapeptide sequence GGGPGGG. The peptide's C terminus was esterified with *n*-heptyl alcohol. The C-terminal capping was done to prevent ionization of the carboxyl group and to provide a secondary membrane anchor for the amphiphilic peptide.[29]

Four compounds (plus a control) that incorporated these essential features were required for this fluorescence study. The parent, control structure is $(C_{18}H_{37})_2$N-CO-CH_2OCH_2CO-$(Gly)_3$-Pro-$(Gly)_3$-$O(CH_2)_6CH_3$ (**1**). Fluorescent residues were incorporated at the C terminus (seventh amino acid position) in two of the structures by replacing glycine with L-glutamic acid ($G^7 \rightarrow E^7$) that had been esterified by 1-pyrenemethanol to give **2** or by L-tryptophan ($G^7 \rightarrow W^7$) to give **3**. In compound **4**, lysine replaced the glycine at position 5 ($G^5 \rightarrow K^5$, that is, GGGPKGG), and the terminal amine was dansylated. Similarly, a C-terminal lysine was attached to nitrobenzodioxazole (NBD)[30] to give the fluorescent derivative **5**.

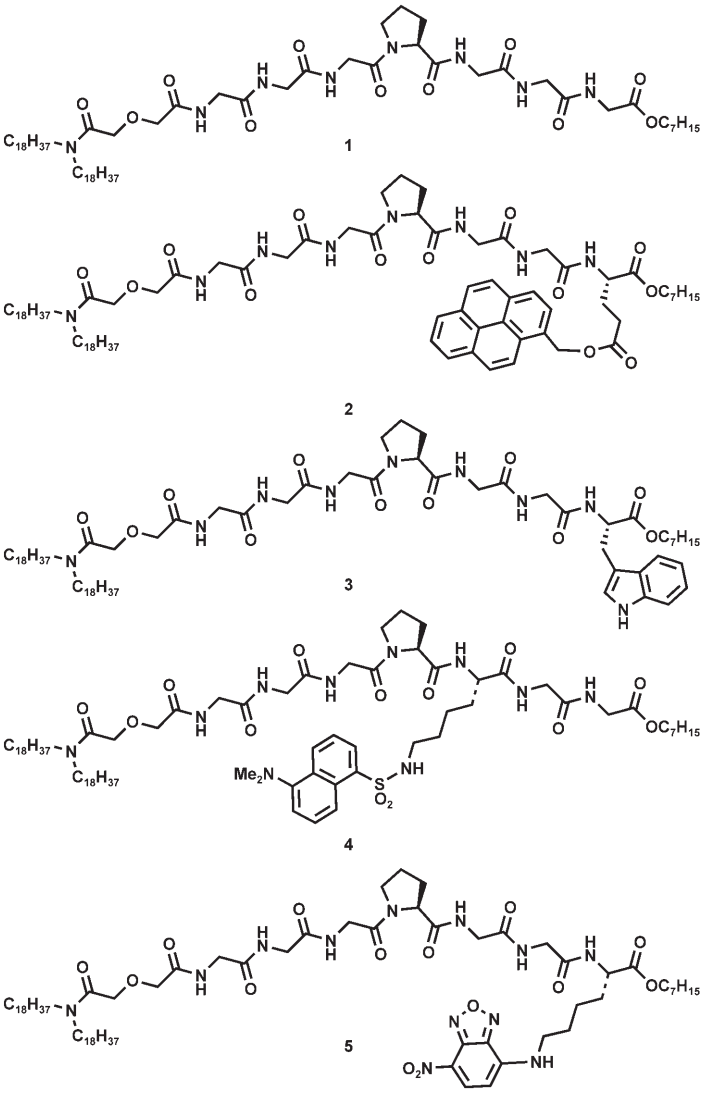

The preparation of each amphiphilic peptide was accomplished by a general scheme that has been previously described.[29] In brief, diglycolic anhydride was heated with dioctadecylamine to give $(C_{18}H_{37})_2NCOCH_2OCH_2COOH$ (18_2-[DGA]OH). Commercial triglycine benzyl ester was coupled to this acid to give $(C_{18}H_{37})_2NCOCH_2OCH_2CO$-Gly-Gly-Gly-OH after debenzylation. The acid was then coupled with the appropriate tetrapeptide (e.g. H-Pro-$(Gly)_3$-O-

$(CH_2)_6CH_3 \rightarrow$**1**) to produce the desired compound. The preparations of previously unreported structures are recorded in the Experimental Section.

Attempts to directly attach the NBD residue to the lysine amino group in 18_2[DGA]GGGPGGK-OC_7H_{15} were unsuccessful. Thus, NBD was coupled with the side-chain amine of Boc-L-lysine[31] to place NBD on the ε-amine. The product was directly esterified without purification. Removal of the *tert*-butyloxycarbonyl (Boc) group, followed by coupling with 18_2[DGA]-GGGPGG-OH afforded compound **5**. Scheme 1 shows the sequence used for the successful preparation of **5**.

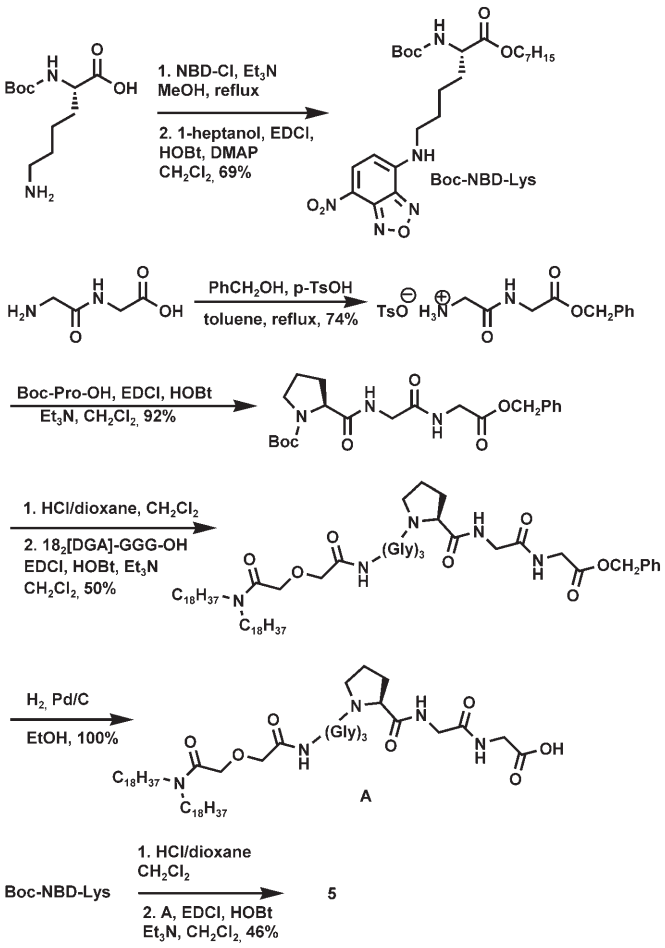

Scheme 1. Preparation of compound **5**. DMAP = 4-dimethylaminopyridine; EDCI = 1-ethyl-3-(3-dimethylaminopropyl)carbodiimide; HOBt = 1-hydroxy-1*H*-benzotriazole.

Chloride release from liposomes mediated by compounds 1–5: The ability of **1** and its analogues to selectively[24,28b] transport Cl^- has been demonstrated previously.[32] It was necessary to demonstrate that in **2**–**5**, the fluorescence probes that were incorporated into the peptide sequence did not fundamentally alter the transport behavior. The fact that transport behavior is similar in the labeled and nonlabeled peptide amphiphiles strongly suggests, although it does not prove, that the fluorescent probe is not fundamentally altering behavior. This determination is especially important for fluorescent labels, which often are rather large entities that can influence local membrane structure and organization.

The transport experiments were conducted as follows. Liposomes (~200 nm in diameter) were prepared from a mixture of 1,2-dioleoyl-*sn*-glycero-3-phosphocholine (DOPC) and 1,2-dioleoyl-*sn*-glycero-3-phosphate (DOPA) (7:3 (w/w)), as described in the Experimental Section. The liposomes encapsulated 600 mM KCl in HEPES buffer (pH 7), and the chloride-free external buffer was 400 mM K_2SO_4 in HEPES (pH 7). An Accumet chloride combination electrode was calibrated by using an aqueous KCl standard. The electrode was then introduced into the suspension and the vesicle system was checked for leakage. In each case, the ionophore under study was then introduced in minimal 2-propanol, and the electrode response was recorded. Experiments were typically conducted for 1800 s, and the final Cl^- concentration was determined by vesicular lysis. The Cl^- release data are shown for **1**–**5** in Figure 1.

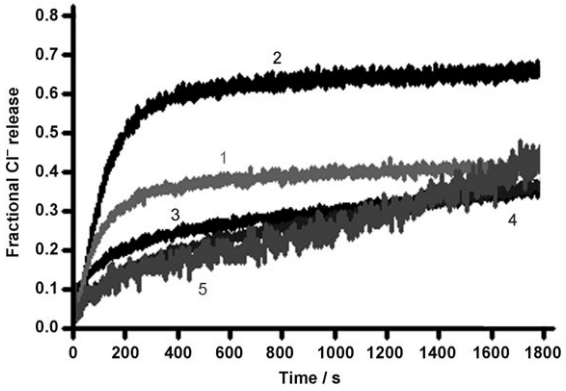

Figure 1. Chloride release from liposomes mediated by **1**–**5** (0.31 mM lipids, 65 μM compounds, pH 7).

Each of the data lines represents the average of at least three independent assays. The data reproducibility is acceptable for all five compounds and is excellent for **1**–**4**. A slightly greater variation was observed for NBD-derivative **5** although good Cl^- release dependence on the concentration of **5** was observed over the range 22–108 μM. The chloride release activity data (Figure 1) shows that pyrene derivative **2** is a more effective mediator of Cl^- release than the other four compounds. Compound **1** is more effective at shorter times, but **1** and **3**–**5** all release about 40% of the available Cl^- ion within 1800 s. The differences in transport efficacy are likely due to a combination of placement and identity of the fluorescent residue. The variation cannot be due only to the position of the amino acid within the peptide because the dansyl-terminated lysine is in amino acid position 5, whereas the other four compounds differ at the C terminus (position 7). Notwithstanding some differences in the release curve shape and in transport efficacy, compounds **1**–**5** all mediate Cl^- release.

Pyrene steady-state fluorescence: Pyrene is an excellent probe of aggregation because the proximity of the two arene residues leads to a fluorescent excimer. When pyrene is uniformly dispersed in a solvent, such as ethanol, excitation (λ_{exc}) at 345 nm gives a spectrum that exhibits two prominent peaks at $\lambda \sim 375$ and 395 nm. In contrast, when two pyrenes associate to form an excimer, irradiation leads to the observation of a broad band that is centered at approximately 472 nm.

The fluorescence of pyrenyl ester **2** was recorded in aqueous HEPES buffer, EtOH, or CH_2Cl_2 after excitation (λ_{exc}) at 345 nm. Fluorescence peaks ($\lambda \sim 375$, 395 nm) that indicate the presence only of monomer were observed in CH_2Cl_2 and EtOH. In aqueous HEPES buffer, however, the pyrene excimer peak ($\lambda \sim 472$ nm) predominated. The peak shapes and positions observed in organic and aqueous solvents comport with self-assembly or aggregation of **2** in buffer. No excimer band was detected under comparable conditions either in organic solvents or in aqueous solution for 1-pyrenylmethanol alone. Thus, aggregation is fostered by self-assembly of the peptide amphiphile and not by pyrene itself. The ability of nonfluorescent **1** to self-assemble was demonstrated by titrating pyrene derivative **2** with **1**. In this case, pyrenyl monomer fluorescence increased as the amount of **1** increased (see the Supplementary Information).

The fluorescence spectra of **2** were also obtained in vesicular suspension. No monomer peak was apparent when the fluorescence spectrum of **2** was obtained in HEPES buffer. In either DOPC/DOPA (7:3) or DOPC liposome suspensions, however, both monomer and excimer peaks were observed (Figure 2). Peptide **2** aggregates rapidly in aqueous solution. These dimers or oligomers then contact the liposome surface and partition into the membrane. The observation of pyrene monomer fluorescence in the bilayer indicates that aggregates that are formed in buffer must dissociate during or after peptide insertion and subsequent pore formation. The fluorescence intensity change for pyrene monomer/excimer is a sensitive index for peptide aggregation and insertion.

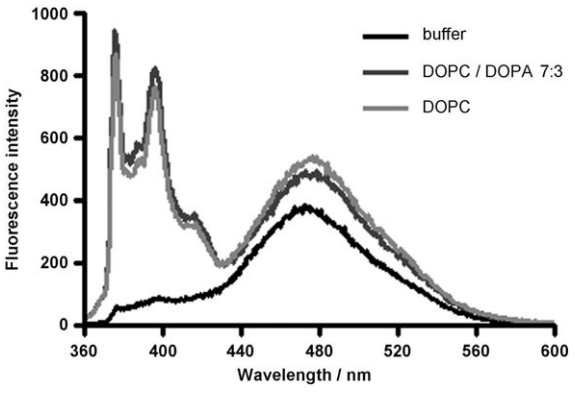

Figure 2. Fluorescence spectra of **2** (1.84 μM) in liposomes (0.31 mM) suspended in HEPES buffer and in buffer.

Position of a SAT within the liposomal bilayer assessed by dansyl and indole fluorescence: The tryptophan indole of **3** and the dansyl group of **4** both exhibit solvent-dependent fluorescent shifts. The fluorescence spectra of dansyl-containing **4** were recorded in solvents of different polarities and in liposomal (aqueous) suspension. Figure 3 plots the position of the longest wavelength peak as a function of E_T.[33] The solvent polarity parameter E_T is determined directly by spectral measurements in the solution and, therefore, correlates better than does the solvent dielectric constant with the fluorescence measurements reported here.[34] The emission maximum increases as the solvent polarity increases linearly (slope = 1.19, $r^2 = 0.97$).

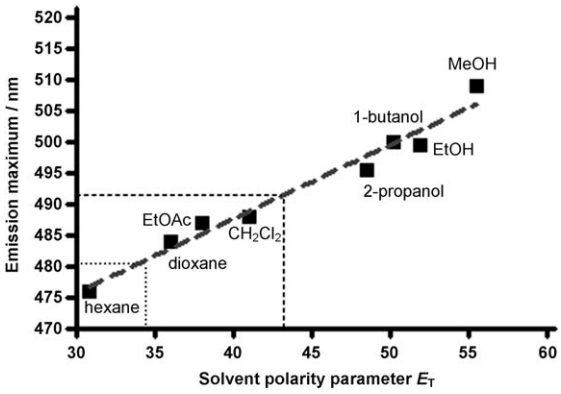

Figure 3. Plot of fluorescence emission maxima for **4** ([**4**] = 4.95 μM) in solvents of differing polarity. ••••• and ----- correspond, respectively, to **4** in HEPES buffer and to DOPC/DOPA liposomes.

The fluorescence maximum observed for dansyl-containing peptide **4** in HEPES buffer was 481 nm (••••• in Figure 3). This corresponds to an E_T value of ~35 and suggests that the dansyl residue experiences an environment that is intermediate in polarity between hexane and dioxane. The dielectric constant (ε, which is generally more familiar than E_T) for aqueous buffer is ~80, and for dioxane it is ~2.[35] The striking difference between the polarity expected for a dansyl group in aqueous solution and the value observed here strongly suggests that **4** self-assembles in buffer. These results are consistent with those found for pyrenyl peptide **2**, as described above.

The same dansyl-containing peptide **4** was then added to an aqueous liposomal suspension (DOPC/DOPA, see the Experimental Section). The fluorescence maximum was observed at $\lambda = 492$ nm (----- in Figure 3). Interpolation gave an E_T value of ~44, which is between the E_T values for CH_2Cl_2 and 2-propanol. If the heptapeptide comprises the entry portal of a dimeric (or larger) pore assembly and the dansyl group extends into the membrane from the peptide chain, the sulfonyl group will be about 9 Å deep. The depth of the midpolar (glyceryl) regime is similar, which suggests that the naphthalene residue is infiltrating the hydrocarbon/insulator segment of the membrane.

The relevant Reichardt polarity scale ranges from 63.1 for H_2O to about 33 for xylenes.[34] This scale is appropriate for the present work, but the correlation with the more familiar dielectric constant (ε) is problematic. Table 1 shows a comparison of E_T and ε values. If one considers the solvent functional groups that interact directly with the solute as being reflected in E_T, the disparity with the bulk solvent dielectric constant is less troubling. In any event, it is clear that the dansyl residue of **4** experiences an environment that is significantly less polar than water and more polar than xylene, which is presumably close to the bilayer's hydrocarbon insulator regime. At the least, we infer that the dansyl side chain of compound **4** resides within the bilayer rather than being in contact with water.

Table 1. Comparison of E_T and dielectric constants.

Compound	ε	E_T
p-xylene	2.27	33.2
CH_2Cl_2	8.93	41.1
DMF	37.0	43.8
3 or **4**[a]	–	~44
*i*PrOH	19.9	48.6
EtOH	24.6	51.9
H_2O	78.4	63.1

[a] The E_T-defined environment that is experienced by **3** or by **4** in bilayer.

Similar measurements were conducted for indole-containing compound **3** and, as with **4**, a straight line was obtained (slope = 0.53, $r^2 = 0.91$, see the Supporting Information). The slope is shallower because indole is a less-fluorescent residue than is dansyl. When **3** was added to an aqueous suspension of DOPC/DOPA liposomes, excitation at $\lambda =$ 283 nm resulted in an emission at $\lambda = 343$ nm. This interpolates to a polarity between CH_2Cl_2 and 1-butanol; the corresponding E_T value is about 44. The indole residue of **3** is, therefore, in the same polarity regime as the dansyl group of **4**, that is, it is in a portion of bilayer that has intermediate polarity.[36]

Fluorescence resonance energy transfer (FRET): The indole residue in tryptophan-containing peptide **3** absorbs energy at $\lambda = 283$ nm and fluoresces at $\lambda = 340$ nm. The pyrenyl residue of amphiphile **2** absorbs at 345 nm. If compounds **2** and **3** aggregate to form a pore, fluorescence resonance energy transfer (FRET) should be observed. If **2** is behaving as a monomer, a band with two prominent peaks at $\lambda = 375$ and $\lambda = 395$ nm will be apparent. If two molecules of **2** are close enough to interact and form an excimer, energy transfer from **3** will result in a broad band emission centered at $\lambda =$ 472 nm. If **2** and **3** behave independently, no FRET will be apparent.[37–39] We note that a mixture of **2** and **3** mediates Cl^- release from DOPC/DOPA liposomes (data not shown).

Three experiments were conducted that were essentially identical except for the solvents in which they were run. The results are shown in the three panels of Figure 4. The solvents were aqueous HEPES buffer, anhydrous EtOH, and aqueous liposomal suspension. In each case, the sample was excited at $\lambda = 283$ nm and the emission spectrum was recorded over the wavelength range of 250–600 nm. The traces in Figure 4 show the results for **2** alone (light gray), **3** alone (dark gray), and an equimolar mixture of **2** and **3** in black. The final concentrations of the individual component are the same.

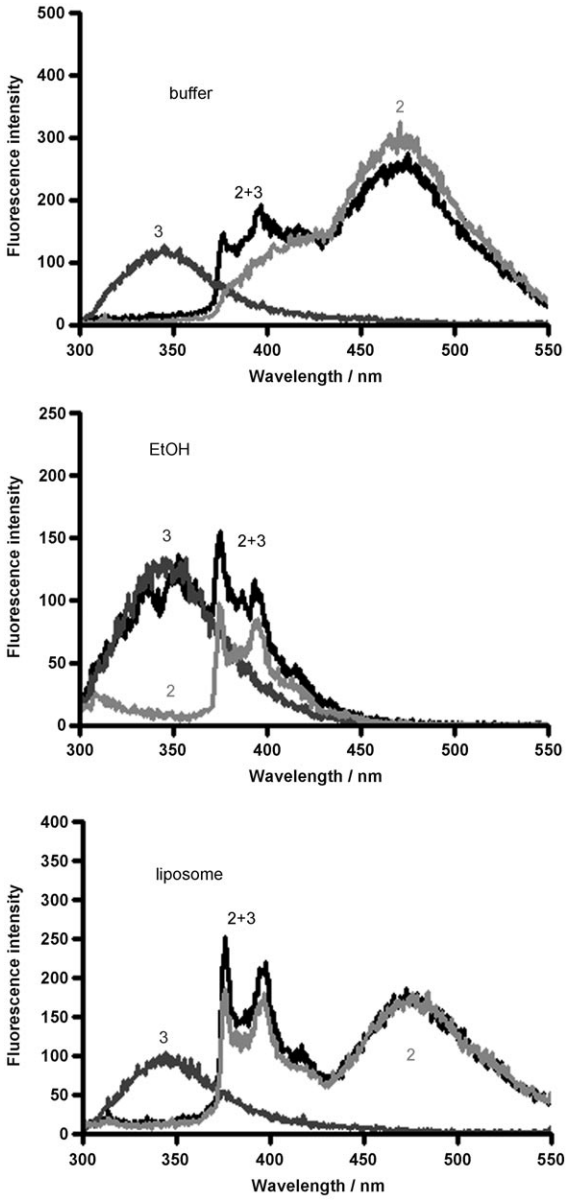

Figure 4. Fluorescence resonance energy transfer (FRET) between **2** and **3** in (top) buffer, (middle) EtOH, and (bottom) liposomal suspension. The concentrations were individual, [**2**] = [**3**] = 2.47 μM; mixed, [**2+3**] = 4.94 μM; and [lipid] = 310 μM.

The top panel of Figure 4 shows that in HEPES buffer, the fluorescent emission of indolyl amphiphile **3** (dark gray trace) is observed as a band with a maximum near 340 nm. Compound **2**, alone in HEPES buffer (light gray trace), shows the characteristic excimer band near 472 nm. The 340 nm band of **3** disappears when an equivalent amount of

2 is added. Thus, energy transfer (FRET) must occur between the indole of **3** and the pyrene of **2**, leaving no residual emission spectrum of **3**. The monomer emission (two peaks, 375–400 nm) for pyrenyl peptide **2** increases in intensity when a mixture of **2** and **3** are present; this suggests that **2**·**3** is forming. Taken together, these experiments show that compounds **2** and **3** aggregate (co-assembly) in aqueous buffer solution.

Compounds **2** and **3** are soluble in EtOH. The middle panel of Figure 4 shows that the individual spectra of **2** and **3** are essentially additive in this solvent and no FRET is apparent. This is expected because the peptides are soluble in EtOH and are expected to be distributed throughout the organic solvent with no driving force for association.

The bottom panel of Figure 4 shows the fluorescence spectra for a mixture of **2** and **3** in a DOPC/DOPA liposomal suspension. The dark gray trace shows the expected fluorescence spectrum of indole in **3**. When **2** is present in liposomes (light gray trace), both monomer and excimer peaks are apparent in the fluorescence spectrum. When pyrene-containing **2** is mixed in equimolar proportion with indole-containing **3**, the indole fluorescence is lost. The fluorescence emission energy from the indole in **3** is clearly transferred to pyrene in **2**. We note that the fluorescence spectra for **2** and **2**+**3** (black trace) are nearly superimposable.

Although ionophores **2** and **3** are likely partitioned between the liposomes and the aqueous buffer, the overall effect is complete quenching of the indole fluorescence. The extent of insertion of SATs into the phospholipid (liposomal) bilayer was assessed (see details below) by using NBD peptide **5**. By using the partition data obtained for **5**, and by assuming that the partition for **2** and **3** is similar, then the fraction of peptide in the bilayer is 94% for **2** and **3** and 88% for the mixture of **2** with **3**. Therefore, nearly all of the monomers (**2** and **3**, or their mixture) reside within the bilayer during the FRET experiment. The observation of energy transfer between the indolyl (e.g. **3**) and pyrenyl (e.g. **2**) residues confirms insertion and shows that these residues must be proximate within the bilayer. We infer that the ionophores partition from the buffer into the liposomal bilayer. Once in the bilayer, the ionophores (in this case **2** and **3**) aggregate and self-assemble with concomitant formation of an active pore. This inference is consistent with previously reported carboxyfluorescein release experiments.[28b,29] Hill plots in those cases indicated that the pores that are formed by **1**, and its relatives are at least dimeric. We note that chloride and carboxyfluorescein anions are different and their transport behavior does not always correlate.[17] The FRET studies that are presented here provide direct experimental evidence for SAT assembly in the bilayer membrane. The observation of FRET between the indole of **3** and the dansyl of **4** in buffer and in liposomal suspension, but not in EtOH, confirms this (see the Supporting Information).

Fluorescence-quenching studies: Acrylamide (CH_2=CH-$CONH_2$), is a molecule that is known to function as a fluorescence quencher.[40,41] How effectively acrylamide quenches a fluorophore gives information about the distance relationship between the two. After the synthetic peptides are added to an aqueous liposomal suspension, they reside in the aqueous buffer, on the liposomal surface, or within the liposomal bilayer. Acrylamide was, therefore, added to the same suspension and the changes in both pyrene (**2**) and indole (**3**) fluorescence were assayed.

In four separate experiments, pyrene-containing **2** and indole-containing **3** in HEPES buffer or DOPC liposomal suspension were titrated with aqueous acrylamide solution. In each case, the fluorescence emission spectra of **2** or **3** ([**2**] = 1.87 μM, [**3**] = 4.95 μM) were recorded whereas the amount of acrylamide was increased. The efficacy of quenching is determined by several factors. As the concentration of quencher increases, the observed luminescence decreases. The Stern–Volmer equation ($F_0/F = 1 + k_{SV}[Q]$, k_{SV} is the quenching constant and [Q] is the quencher concentration) was applied to the quenching data and non-linear plots were obtained in both buffer and vesicles. From the results described in the sections above, it was clear that the peptide amphiphiles aggregate in aqueous buffer and that the active pore forms by a self-assembly process within the bilayer. Such aggregation likely causes a fraction of the fluorophore to be inaccessible to quencher. We, therefore, applied the modified Stern–Volmer analysis[42,43] (shown in Figure 5), which takes account of the fraction of fluorophore that is inaccessible to quencher. In this case, all plots were nicely linear for compounds **2** and **3**, either in buffer or liposome suspension.

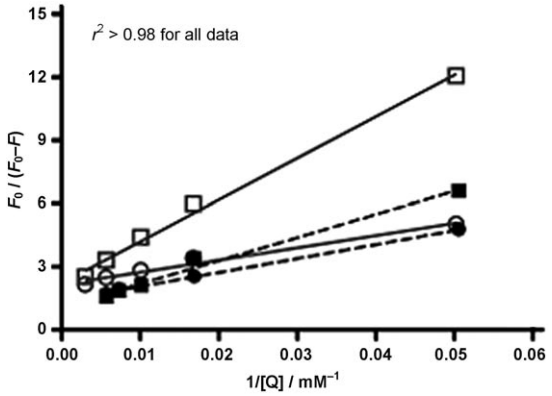

Figure 5. Modified Stern–Volmer treatment of the quenching data for **2** and **3**. □: **2** in buffer (data fit: ——), ○: **2** in DOPC (——); ■: **3** in buffer (-----), ●: **3** in DOPC (-----). All linear regressions fit with $r^2 > 0.98$. [**2**] = 1.87 μM, [**3**] = 4.95 μM.

The plots shown in Figure 5 were analyzed and the quenching data extracted are summarized in Table 2. The term f_a is the fraction of fluorophore accessible to quencher and k_a is the apparent quenching constant. The fraction of indole residues (**3**) that are accessible to acrylamide approaches unity in buffer and is 0.7 in the DOPC membrane. The pyrene residue of **2**, however, is much less accessible to

Table 2. Quenching data for compounds **2** and **3**.

	f_a[a]		k_a [M^{-1}][b]	
Compound	Buffer	DOPC	Buffer	DOPC
2	0.449	0.465	11.3	36.8
3	0.919	0.712	9.9	21.2

[a] Fraction of fluorophore accessible to acrylamide. [b] k_a is the apparent quenching constant.

quencher in either medium. Indole is a hydrogen-bond donor (N–H) and can serve as a headgroup in amphiphiles.[44] It seems reasonable that the smaller, H-bonding indole of **2** would be more accessible to quencher than the larger, more hydrophobic pyrene of **3** in either medium. The apparent quenching constant, k_a, is larger in DOPC liposomes than it is in external buffer for both peptides. A smaller quenching constant is expected for larger aggregates. Moreover, acrylamide is a small molecule that can readily infiltrate the conducting pores and could directly quench membrane-buried residues.

Partition and insertion of SATs into the bilayer: As noted above, addition of amphiphilic SATs to an aqueous liposome suspension engenders a complex dynamic. The amphiphiles can aggregate in the buffer, adhere to the liposomal bilayer, insert in the bilayer, and diffuse within the bilayer to form functional pores. We wished to quantify the membrane partition process and, therefore, prepared compound **5** (see above), which contains the fluorescent label 7-nitrobenz-2-oxo-1,3-diazole (NBD). This label is relatively small and highly fluorescent, making it ideal for the present study. It was essential, however, to demonstrate that transport efficacy was not compromised by its presence. The efficacy of **5** in mediating Cl^- release was studied and found to be concentration dependent in the range 22–108 μM (see the Supporting Information).

The NBD fluorophore is valuable as a membrane probe because its fluorescence intensity is greater within the bilayer than it is in aqueous solution owing to water quenching in the latter. In control experiments, the fluorescence emission spectra of **5** ($\lambda_{exc}=465$ nm) were recorded in various solvents, but almost no fluorescence emission was observed in aqueous buffer. The ability of NBD-containing SAT **5** to partition into the liposomal bilayer was evaluated as follows. Vesicles that encapsulate potassium chloride were prepared from a 7:3 mixture of DOPC and DOPA. The liposomes were suspended in potassium sulfate buffer, **5** (4.95 μM) was added, and NBD fluorescence was observed at $\lambda=535$ nm ($\lambda_{exc}=465$ nm) during 1000 s. The amount of lipid (as liposomes) added was increased from its initial value of 15.4 to 512 μM, as shown in the graph of Figure 6. This gave an overall [lipid]/[**5**] range of ~3–100.

The graph of Figure 6 demonstrates that longer equilibration times are required at higher [lipid]/[**5**] ratios. Below a [lipid]/[**5**] ratio of 6.90 (the fourth line from the bottom in Figure 6), **5** reaches a lipid–buffer equilibrium fairly rapidly. We interpret this to mean that although there is a large excess of lipid compared to **5**, there is still insufficient lipid to accommodate all of the available **5** within the liposomal bilayers. As the vesicle concentration increases, more peptide can partition into the bilayer but more time is also required to reach equilibrium. In fact, when [lipid]/[**5**] >6.90, equilibrium was not reached in the arbitrarily set time frame of the experiment (Figure 6).

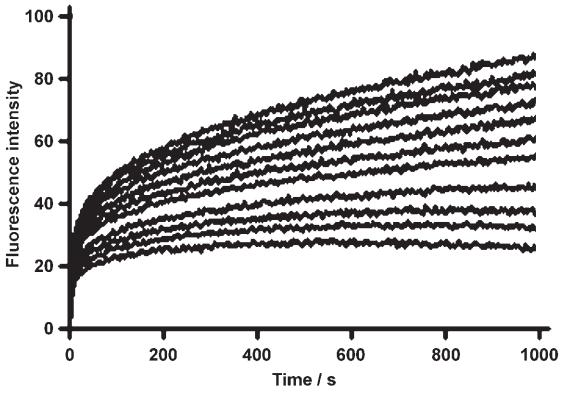

Figure 6. NBD fluorescence intensity change during chloride release from DOPC/DOPA (7:3) vesicles (15.4–512 μM). [**5**]=4.95 μM. NBD was excited at $\lambda=465$ nm and emission was recorded at $\lambda=535$ nm.

The data reported above permitted a semiquantitative assessment of peptide partition between buffer and bilayer.[45] SAT aggregates in aqueous buffer and this monomer/aggregate equilibrium complicates its partition process. We also noted above that an equilibrium was not established at higher lipid concentrations within the 1000 s duration of Figure 6. We, therefore, chose to compare values at the 900 s time point in the following analysis as a simplified model to estimate the partition coefficient. First, $F-F_0$ was graphed as a function of lipid concentration; this gave the expected hyperbolic curve (analysis shown below in Figure 7). The variables F and F_0 refer to fluorescence intensities in the presence and absence of lipid, respectively. The value of F_0 was 5.20 at 900 s.

The partition constant K_p was obtained from the straight-line plot ($r^2=0.99$) of $1/(F-F_0)$ versus 1/[L] (Figure 7),

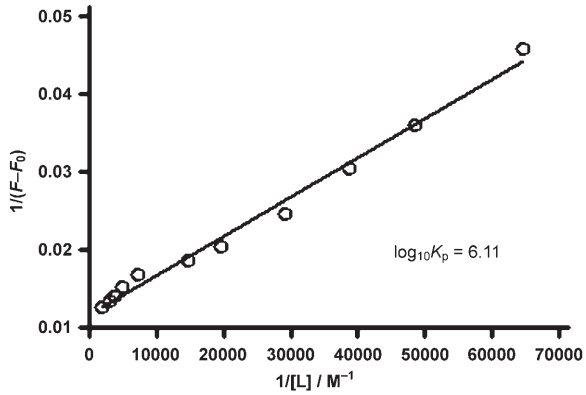

Figure 7. Treatment of partition data for **5**. $1/(F-F_0)$ was plotted against 1/[L] and a straight line was obtained, $\log K_p=6.11$.

$\log K_p = 6.11$. In the analytical approach used here, 900 s is not an equilibrium point at higher [L]/[**5**] values. Thus, the actual value of K_p should be larger than is apparent. In a typical Cl^- release experiment conducted in our laboratory, the [lipid]/[compound] ratio is 4.77 ([L] = 310 μM, [compound] = 65 μM). By applying the above-determined values, we can estimate that at least 35% of the available SAT inserts into the liposomal bilayer. Thus, the Cl^- release experiments typically reflect the activity of only about a third of the available ionophores.

Quenching of NBD fluorescence: The ionophoric peptides described here are added to the aqueous suspension and, therefore, contact the outer leaflet of the bilayer first. Cumulative evidence suggests that they insert into the bilayer and form a transmembrane pore. The question addressed here is whether these peptides remain in the outer leaflet or translocate and populate both leaflets of the bilayer. Such a flip–flop process can be monitored by using an NBD/dithionite quenching assay. Sodium dithionite ($Na_2S_2O_4$) reduces the NBD nitro group and thus quenches its fluorescence. The phospholipid bilayer is impermeable to $Na_2S_2O_4$ so only the NBD-labeled peptide present in the outer leaflet is quenched.

Titration experiments similar to those above were conducted except that the $Na_2S_2O_4$ solution in Tris buffer was added after about 10 min. Typical results are shown in Figure 8 and the results of control experiments (no quencher) are included for comparison. After dithionite addition, NBD fluorescence intensity decreased dramatically followed by very slow decay. One concern is that $S_2O_4^{2-}$ could migrate through chloride-transporting pores formed by peptide dimerization. However, compared to 2 mL of 400 mM K_2SO_4 buffer, 25 μL of 600 mM $Na_2S_2O_4$ is a negligible quantity. Moreover, sulfate is not transported well across the bilayer as previously demonstrated.[24b] We conclude from these dithionite quenching experiments that the ionophoric peptide is located predominantly in the bilayer's outer leaflet and that flip–flop of the membrane bound peptide is slow.

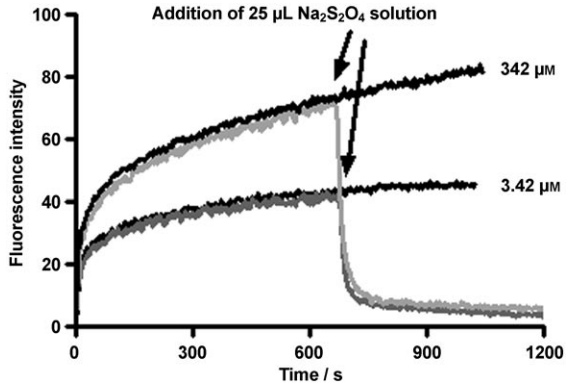

Figure 8. Quenching of NBD fluorescence by $Na_2S_2O_4$ (600 mM in 1 M Tris buffer, pH ~ 10). [**5**] = 4.95 μM. NBD was excited at 465 nm and emission was recorded at 535 nm. Two trials were conducted with [L] = 3.42 and 342 μM.

By using the NBD fluorescence data that are described above, the partition coefficient K_p was found to be 1.29×10^6. The parameter K_d^{eff} is the effective dissociation constant that represents the concentration of exposed lipids at which the peptide is 50% partitioned into the bilayer. This value was found to be ~43.0 μM. A high affinity value would be $K_d^{eff} < 1$–2 μM, so we characterize the SATs as having modest membrane affinity. In chloride release (ISE) measurements ([L] = 310 μM, [compound] = 65 μM), the fraction of SAT that inserted into the bilayer was at least 35%. Unfortunately, SAT partition and pore activation are indistinguishable from each other because insertion is a slow process (see Figure 6). Therefore, the fractional chloride release data described here and in previous studies does not reflect the net anion-transporting ability of these molecules. The transport efficacy is actually higher; the release of ions is diminished by insertion dynamics.

Figure 1 shows that although Cl^- release mediated by **2** is better than for **3**, the latter is nearly identical to **5** in transport efficacy. There are admittedly differences in size, shape, and polarity among **2**, **3**, and **5** but they are more similar than different and all three compounds transport Cl^- with reasonable efficacy. We thus assume here that the fraction of each compound that inserts into the bilayer is similar. Absent data to the contrary, this seems to be a reasonable supposition. Based on this assumption, we calculate the fraction of **2** or **3** that inserts in the DOPC/DOPA liposomal bilayer to be at least 35% during the Cl^- release experiments. The latter experiments are run at a higher SAT concentration than the fluorescence experiments, owing to a lower sensitivity of the chloride-selective electrode compared to fluorescence.

Fluorescence microscopy: Optical fluorescence microscopy was used to visualize the location of NBD-SAT **5** in giant unilamellar vesicles (GUVs).[46] Because large vesicles were required for optical visualization, the (GUV) vesicles used in this study were prepared[47] from DOPC rather than from a DOPC/DOPA mixture. The NBD-containing SAT compound (**5**) was incubated with an aqueous suspension of GUVs and both transmitted light and fluorescence images were recorded. Figure 9 shows the images of vesicles in grayscale. The bright spots in the GUV boundary layer clearly indicate the localization of SAT into membrane.

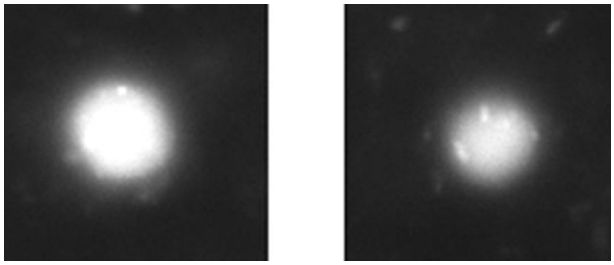

Figure 9. Fluorescence microscopy images of GUVs incubated with **5** are shown in grayscale (two vesicles shown, left and right, respectively).

Conclusion

Synthetic peptides with the general formula $(C_{18}H_{37})_2$N-CO-CH_2OCH_2CO-$(Gly)_3$-Pro-$(Xxx)_3$-OR mediate chloride release from liposomes. Replacement of a glycine by tryptophan, the pyrenylmethyl ester of glutamic acid, dansyl, or by NBD-terminated lysine affords peptides that are comparable in transport efficacy to the parent compound. The fluorescence studies presented here provide direct experimental evidence for the assembly properties of this family of peptide-based synthetic anion transporters in liposomal bilayers.

Taken together, we infer the following about SAT aggregation and function in a phospholipid bilayer membrane. First, the dansyl residue of lysine in **4** resides in a regime of the bilayer that is of intermediate polarity. This means that it is neither embedded in the hydrocarbon-like insulator regime nor is it in contact with water. This is also the case for indolyl derivative **3**. These results support our previous surmise that the peptide served as a headgroup positioned near the top of the upper bilayer leaflet. Second, pyrene monomer/excimer fluorescence is a sensitive index for peptide insertion into the bilayer. Only the excimer peak was apparent for **2** in buffer whereas both monomer and excimer were observed in lipid suspension. Thus, dissociation must occur for an active pore to form. It is currently unclear whether an aggregated species inserts in the bilayer and rearranges to form the pore or if monomers insert and the aggregates subsequently form a pore within the bilayer. Indeed, both may occur. Third, when both indole and pyrene are present in different amphiphilic peptides, FRET is observed; this indicates that the two different monomers can assemble into an active pore. Fourth, fluorescence quenching by acrylamide in both aqueous buffer and liposomal suspension confirmed that the fluorophore experienced different environments in these media.

The NBD fluorescence studies reveal two important points. First, the insertion of SAT into the bilayer is slow. This means that the pore formers are more effective at ion release than is apparent from the release data. Second, quenching of NBD fluorescence indicates that the SAT resides (remains) in the outer leaflet of membrane; no translocation is apparent.

The data obtained in the present study provide critical information about this family of synthetic, anion-transporting ionophores. These studies confirm the self-assembly of peptide monomers within bilayers. We have shown that at higher concentrations, only a fraction of the available amphiphiles insert in the bilayer and the peptide headgroup resides in the portion of bilayer that has an intermediate polarity. There is no evidence from the present study that transverse relaxation (flip–flop) of the SAT monomers occurs. This confirms the previous structural assumption concerning pore formation, namely that the lower leaflet headgroups reorient to provide part of the conduction pathway.[48,49] Overall, the results reported here supply a mechanistic model for this family of synthetic anion transporters.

Experimental Section

Vesicle preparation and chloride release experiment: Chloride release was assayed directly on ~200 nm phospholipid vesicles prepared from 7:3 1,2-dioleyl-*sn*-glycero-3-phosphocholine (DOPC) and 1,2-dioleyl-*sn*-glycero-3-phosphate monosodium salt (DOPA, both from Avanti Polar Lipids) by using a chloride-selective electrode (Accumet Chloride Combination Electrode). Vesicles were prepared in the presence of an internal, chloride-containing buffer (600 mM KCl, 10 mM HEPES, adjusted to pH 7). After extrusion and exchange of external solution with a chloride-free buffer (400 mM K_2SO_4, 10 mM HEPES, pH 7), vesicles were suspended in the same external buffer (final phospholipid concentration about 0.31 mM). The electrode was introduced into the solution and allowed to equilibrate. The voltage output was recorded, and after 5 min, aliquots of the solution of compound at study (9 mM in *i*PrOH) were added. Complete lysis of the vesicles was induced by the addition of a 2% aqueous solution of Triton X-100 (100 μL) and the collected data were normalized to this value. The data were collected by Axoscope 9.0 by using a Digi-Data 1322 A series interface.

Fluorescence spectroscopy: Fluorescence was measured by using a Perkin–Elmer LS50B fluorimeter to evaluate continuously stirred samples. A stock solution of 0.50 mM fluorescent channel in *i*PrOH was prepared. Compound was added, and the solution was stirred for about 60 s before the spectra were recorded. Except where indicated in the text or figure captions, the emission spectrum was measured in external buffer (2 mL, 400 mM K_2SO_4, 10 mM HEPES, pH 7.0). For solvent-dependence experiments, freshly distilled solvent (2 mL) instead of buffer was used and the concentration was adjusted for the instrument capacity. For the measurement in the vesicles, compound was added to the liposome suspension (as prepared above) in external buffer (2 mL) and the overall lipid concentration was 0.31 mM (same as for the chloride release experiment). For FRET experiments, the excitation wavelength was 283 nm and the emission spectrum was recorded between 250–600 nm (2.5 nm slit width, 400 nm min^{-1} scan speed, average three scans). The compound solution was mixed together before the addition to the cuvette. In the quenching experiments, 8 M aq acrylamide was added in small aliquots so that the fluorophore concentration was not dramatically affected.

NBD-peptide partition and quenching: DOPC/DOPA (7:3) vesicles were prepared as described above. Vesicle-titration experiments were conducted in 400 mM K_2SO_4, 10 mM HEPES (pH 7) buffer. The total volume of buffer and liposome suspension was 2 mL, which was initially placed in cuvette and stirred. Compound **5** was added (20 μL of a 0.5 mM *i*PrOH solution) to the cuvette through the injection port of fluorimeter. The final concentration of peptide was 4.95 μM. The excitation wavelength was 465 nm and the emission wavelength was 535 nm (2.5 nm slit width, 1 s data interval). The recording lasted at least 20 min. For quenching measurements, a 600 mM $Na_2S_2O_4$ in 1 M Tris buffer solution (25 μL, pH ~ 10) was added to the cuvette about 10 min after the peptide injection and the recording was continued for at least 10 min. Control experiments without quencher were also conducted.

Fluorescence microscope: GUV was prepared from DOPC as reported.[47] The size of GUV was found to be between 5–25 μm as measured by transmitted light imaging. Compound **5** (0.5 mM in 2-propanol) was added to GUV, incubated for 1 h (final **5** concentration around 25 μM) and fluorescence imaging was taken by using Leica DM5000 B optical microscope.

Acknowledgement

We thank the NIH for grants (GM-36162, GM-63190) that supported this work.

[1] A. Bianchi, K. Bowman-James, E. Garcia-España, *Supramolecular Chemistry of Anions*, Wiley-VCH, New York, **1997**, p 461.

[2] J. L. Sessler, P. Gale, W.-S. Cho, *Anion Receptor Chemistry*, Royal Society of Chemistry, Cambridge, **2006**.
[3] F. P. Schmidtchen, M. Berger, *Chem. Rev.* **1997**, *97*, 1609–1648.
[4] P. D. Beer, P. A. Gale, D. K. Smith, *Supramolecular Chemistry*, Oxford University Press, Oxford, **1999**, p 92.
[5] P. D. Beer, P. A. Gale, *Angew. Chem.* **2001**, *113*, 502–532; *Angew. Chem. Int. Ed.* **2001**, *40*, 486–516.
[6] P. A. Gale, *Acc. Chem. Res.* **2006**, *39*, 465–475.
[7] K. Bowman-James, *Acc. Chem. Res.* **2005**, *38*, 671–678.
[8] A. L. Sisson, M. R. Shah, S. Bhosale, S. Matile, *Chem. Soc. Rev.* **2006**, *35*, 1269–1286.
[9] A. P. Davis, D. N. Sheppard, B. D. Smith, *Chem. Soc. Rev.* **2007**, *36*, 348–357.
[10] T. M. Fyles, *Chem. Soc. Rev.* **2007**, *36*, 335–347.
[11] B. A. McNally, W. M. Leevy, B. D. Smith, *Supramol. Chem.* **2007**, *19*, 29–37.
[12] P. V. Santacroce, J. T. Davis, M. E. Light, P. A. Gale, J. C. Iglesias-Sanchez, P. Prados, R. Quesada, *J. Am. Chem. Soc.* **2007**, *129*, 1886–1887.
[13] P. A. Gale, J. Garric, M. E. Light, B. A. McNally, B. D. Smith, *Chem. Commun.* **2007**, 1736–1738.
[14] X. Li, B. Shen, X. Q. Yao, D. Yang, *J. Am. Chem. Soc.* **2007**, *129*, 7264–7265.
[15] a) C. R. Yamnitz, G. W. Gokel, *Chem. Biodiversity* **2007**, *4*, 1395–1412; b) G. W. Gokel, I. A. Carasel, *Chem. Soc. Rev.* **2007**, *36*, 378–389.
[16] N. Sakai, S. Matile, *J. Phys. Org. Chem.* **2006**, *19*, 452–460.
[17] R. Ferdani, R. Li, R. Pajewski, J. Pajewska, R. K. Winter, G. W. Gokel, *Org. Biomol. Chem.* **2007**, *5*, 2423–2432.
[18] A. V. Koulov, T. N. Lambert, R. Shukla, M. Jain, J. M. Boon, B. D. Smith, H. Li, D. N. Sheppard, J. B. Joos, J. P. Clare, A. P. Davis, *Angew. Chem.* **2003**, *115*, 5081–5083; *Angew. Chem. Int. Ed.* **2003**, *42*, 4931–4933.
[19] M. E. Weber, P. H. Schlesinger, G. W. Gokel, *J. Am. Chem. Soc.* **2005**, *127*, 636–642.
[20] B. Hille, *Ionic Channels of Excitable Membranes*; 3rd ed., Sinauer Associates, Sunderland, MA, **2001**, p 814.
[21] H. Schroeder, R. Leventis, S. Rex, M. Schelhaas, E. Nagele, H. Waldmann, J. R. Silvius, *Biochemistry* **1997**, *36*, 13102–13109.
[22] C. C. Forbes, K. M. DiVittorio, B. D. Smith, *J. Am. Chem. Soc.* **2006**, *128*, 9211–9218.
[23] F. Eisele, J. Kuhlmann, H. Waldmann, *Angew. Chem.* **2001**, *113*, 382–386; *Angew. Chem. Int. Ed.* **2001**, *40*, 369–373.
[24] a) P. H. Schlesinger, R. Ferdani, J. Liu, J. Pajewska, R. Pajewski, M. Saito, H. Shabany, G. W. Gokel, *J. Am. Chem. Soc.* **2002**, *124*, 1848–1849; b) P. H. Schlesinger, R. Ferdani, R. Pajewski, J. Pajewska, G. W. Gokel, *Chem. Commun.* **2002**, 840–841.
[25] R. Ferdani, R. Pajewski, J. Pajewska, P. H. Schlesinger, G. W. Gokel, *Chem. Commun.* **2006**, 439–441.
[26] R. Ferdani, G. W. Gokel, *Org. Biomol. Chem.* **2006**, *4*, 3746–3750.
[27] R. Pajewski, R. Ferdani, J. Pajewska, N. Djedovic, P. H. Schlesinger, G. W. Gokel, *Org. Biomol. Chem.* **2005**, *3*, 619–625.
[28] a) L. You, R. Ferdani, G. W. Gokel, *Chem. Commun.* **2006**, 603–605; b) L. You, R. Ferdani, R. Li, J. P. Kramer, R. E. K. Winter, G. W. Gokel, *Chem. Eur. J.* **2008**, *14*, 382–396.
[29] N. Djedovic, R. Ferdani, E. Harder, J. Pajewska, R. Pajewski, M. E. Weber, P. H. Schlesinger, G. W. Gokel, *New J. Chem.* **2005**, *29*, 291–305.
[30] R. S. Fager, C. B. Kutina, E. W. Abrahamson, *Anal. Biochem.* **1973**, *53*, 290–294.
[31] M. Lumbierres, J. M. Palomo, G. Kragol, S. Roehrs, O. Muller, H. Waldmann, *Chem. Eur. J.* **2005**, *11*, 7405–7415.
[32] N. Djedovic, R. Ferdani, E. Harder, J. Pajewska, R. Pajewski, P. H. Schlesinger, G. W. Gokel, *Chem. Commun.* **2003**, 2862–2863.
[33] C. Reichardt, *Chem. Rev.* **1994**, *94*, 2319–2358.
[34] C. Reichardt, *Solvents and Solvent Effects in Organic Chemistry*, 3rd ed., Wiley-VCH, Weinheim, **2003**, p. 629.
[35] G. W. Gokel, *Dean's Handbook of Organic Chemistry*, McGraw Hill Book Company, NY, **2003**.
[36] S. Ohki, K. Arnold, *J. Membr. Biol.* **1990**, *114*, 195–203.
[37] P. R. Selvin, *Methods Enzymol.* **1995**, *246*, 300–334.
[38] R. M. Clegg, *Curr. Opin. Biotechnol.* **1995**, *6*, 103–110.
[39] G. W. Gordon, G. Berry, X. H. Liang, B. Levine and B. Herman, *Biophys. J.* **1998**, *74*, 2702–2713.
[40] M. R. Eftink, *Top. Fluoresc. Spectrosc.* **1991**, *2*, 53–126.
[41] C. M. Cardona, T. Wilkes, W. Ong, A. E. Kaifer, T. D. McCarley, S. Pandey, G. A. Baker, M. N. Kane, S. N. Baker, F. V. Bright, *J. Phys. Chem. B* **2002**, *106*, 8649–8656.
[42] C. M. Samworth, M. D. Esposti, G. Lenaz, *Eur. J. Biochem.* **1988**, *171*, 81–86.
[43] J. D. Tovar, R. C. Claussen, S. I. Stupp, *J. Am. Chem. Soc.* **2005**, *127*, 7337–7345.
[44] a) E. Abel, S. L. De Wall, W. B. Edwards, S. Lalitha, D. F. Covey, G. W. Gokel, *Chem. Commun.* **2000**, 433–434; b) E. Abel, S. L. De Wall, W. B. Edwards, S. Lalitha, D. F. Covey, G. W. Gokel, *J. Org. Chem.* **2000**, *65*, 5901–5909.
[45] J. R. Silvius, F. l'Heureux, *Biochemistry* **1994**, *33*, 3014–3022.
[46] E. Quesada, A. U. Acuna, F. Amat-Guerri, *Angew. Chem.* **2001**, *113*, 2153–2155; *Angew. Chem. Int. Ed.* **2001**, *40*, 2095–2097.
[47] A. Moscho, O. Orwar, D. T. Chiu, B. P. Modi, R. N. Zare, *Proc. Natl. Acad. Sci. USA* **1996**, *93*, 11443–11447.
[48] L. Yang, T. A. Harroun, T. M. Weiss, L. Ding, H. W. Huang, *Biophys. J.* **2001**, *81*, 1475–1485.
[49] H. W. Huang, F.-Y. Chen, M.-T. Lee, *Phys. Rev. Lett.* **2004**, *92*, 198304.

Received: January 24, 2008
Revised: March 21, 2008
Published online: May 15, 2008

